

Coupling between Exciton-Polariton Corner Modes through Edge States

R. Banerjee^{✉,*}, S. Mandal[✉], and T. C. H. Liew[†]

*Division of Physics and Applied Physics, School of Physical and Mathematical Sciences,
Nanyang Technological University, Singapore 637371, Singapore*

 (Received 7 May 2019; revised manuscript received 28 November 2019; accepted 15 January 2020; published 11 February 2020)

Recently realized higher order topological insulators have taken a surge of interest among the theoretical and experimental condensed matter community. The two-dimensional second order topological insulators give rise to zero-dimensional localized corner modes that reside within the band gap of the system along with edge modes that inhabit a band edge next to bulk modes. Thanks to the topological nature, information can be trapped at the corners of these systems, which will be unhampered even in the presence of disorder. Being localized at the corners, the exchange of information among the corner states is an issue. Here we show that the nonlinearity in an exciton polariton system can allow the coupling between the different corners through the edge states based on optical parametric scattering, realizing a system of multiple connectible topological modes.

DOI: [10.1103/PhysRevLett.124.063901](https://doi.org/10.1103/PhysRevLett.124.063901)

Introduction.—Topological insulators (TIs) have attracted attention in the past decade due to their unique exotic property, namely the appearance of backscattering-immune edge states, which can propagate against perturbation without being backscattered. TIs have been explored in various systems including electronics [1,2], photonics [3–10], cold atoms [11,12], exciton-polaritons [13–18], acoustics [19,20], etc. Recently the concept of topological phases was extended to higher order topological phases [21–33] that go beyond the conventional bulk-boundary correspondence [1]. A two-dimensional second order topological insulator can host topologically protected zero-dimensional gapless corner states along with one-dimensional gapped edge states. The zero-dimensional corner states have been realized using quantization of quadrupole moments in square lattices [21,22], classical mechanical systems [26], electromagnetic metamaterials [27,28], breathing kagome lattices [34–36], and acoustic metamaterials [32,37]. Due to the topological properties of these corner states, information can be trapped at the corners of the system, which will be unhampered even in the presence of disorder, making it a potential candidate for information processing [30,38–46]. But corner states, as with other topological modes, are well isolated from each other even in the presence of disorder making it difficult for them to overlap (they are orthogonal eigenstates). Consequently, it is far from obvious whether there are ways in which different corner states can interact. Although information processing necessitates operating with a coupling of multiple modes, the coupling of multiple topological modes is unexplored in the literature (especially for corner states).

In this Letter, we consider theoretically an array of coupled exciton-polariton micropillars arranged in a square

lattice. Exciton-polaritons are hybrid light matter quasi-particles that arise from the strong coupling of quantum well excitons and microcavity photons. They are well known for a variety of nonlinear effects, typically studied in planar microcavities [47,48]. Several experiments were accomplished with arrays of coupled micropillars, where the hopping between two micropillars is realized by having overlap between them [49–54]. These systems have allowed the implementation [16] of schemes [13–15] for first order topological band structures. Theoretical works have studied nonlinear effects in such systems, including inversion of topology [55], formation of solitons [56–58], antichiral behavior [59], and bistability [17].

Here we consider a second order topological polariton band structure, which is based on achieving hopping between sites with opposite sign. This can not be achieved just by varying the overlap between neighboring micropillars, but can be implemented by placing auxiliary micropillars between a main lattice of micropillars. This follows a generic scheme introduced in Ref. [60] for tight-binding lattices, which we verified starting from a particular polariton potential profile. Having established polariton corner states, we study the influence of polariton-polariton scattering, which allows them to couple to edge states. It is via edge states that polariton corner states can interact, where the excitation of one corner state causes excitation of its neighbor, which would not be possible in the linear regime. We have demonstrated a transfer of information encoded in a binary state from one corner to the next, which can occur even in the presence of a realistic level of disorder. We find that the mechanism of information transfer proceeds both faster and with lower required power than the same mechanism considered in a regular non-topological square lattice.

Scheme.—We consider a square lattice of coupled exciton-polariton micropillars as shown in Fig. 1(a). For simplicity, we neglect the spin degree of freedom in the system and consider a single mode of each micropillar, which evolves according to the driven-dissipative nonlinear Schrödinger equation

$$i\hbar \frac{\partial \psi_i}{\partial t} = \left(\Delta - \frac{i\Gamma}{2} + iP \right) \psi_i + \sum_{\langle j \rangle} J_{ij} \psi_j + \alpha |\psi_i|^2 \psi_i - i\alpha_{\text{NL}} |\psi_i|^2 \psi_i + F_i, \quad (1)$$

where Δ is the energy detuning between the polariton mode energy (on site energy) and the laser energy, and Γ is the polariton dissipation. P is a nonresonant pump applied uniformly to all micropillars in the system and as a result the nonlinear loss term α_{NL} is inevitable. α is the strength of nonlinear interaction and F is a coherent driving field (i.e., laser). Next we move to the dimensionless units by making the following transformations: $t \rightarrow t\hbar/J$ and $\psi_i \rightarrow \psi_i \sqrt{(J/\alpha)}$, where J is the weakest hopping amplitude. With these choices Eq. (1) becomes

$$i \frac{\partial \psi_i}{\partial t} = \left(\Delta - \frac{i\Gamma}{2} + iP \right) \psi_i + \sum_{\langle j \rangle} J_{ij} \psi_j + (1 - i\alpha_{\text{NL}}) |\psi_i|^2 \psi_i + F_i, \quad (2)$$

where the polariton-polariton nonlinear interaction is scaled to unity. All the energy terms in the equation are normalized by a factor J , α_{NL} is normalized by α , and $F_i \rightarrow F_i \sqrt{(\alpha/J^3)}$. We consider four different hopping terms ($J, -J, J',$ and $-J'$) realizing the potential described in Fig. 1(a). In writing Eq. (2), we have assumed a tight-binding approximation. Exciton-polaritons can also be modeled directly from a continuous model, discussed in the Supplemental Material [61]. There, we also explain how hopping terms of opposite sign can be achieved, by making use of auxiliary micropillars in the lattice. Although we operate with dimensionless units, we also provide typical real units, corresponding to setting the coupling $J = 1$ meV (corresponding to Ref. [64]).

Neglecting at first the excitation, decay, and nonlinear terms, the energy spectrum (E) as a function of eigenstate quantum number (n) is given in Fig. 1(b). The zero energy modes correspond to the corner states, which are well separated in energy from other modes of the system. This should be expected as, in the absence of nonlinear terms, the model is essentially the same as that applicable to coupled microwave resonators previously shown to exhibit the same topological corner states [28]. Our main aim here is to excite one of the corner modes coherently and couple to other corner modes without affecting the topological property of the system. In this way topological corner modes may be used to store information as well as support

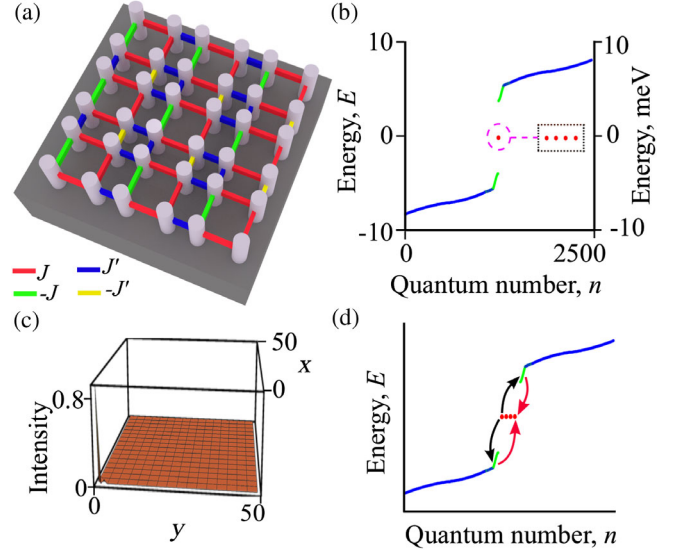


FIG. 1. (a) Schematic diagram of a square lattice formed by coupled exciton-polariton micropillars with four different hoppings, $J, -J, J',$ and $-J'$, indicated by different colors. (b) Energy eigenvalues of the system consisting of 50×50 micropillars, as a function of the quantum number n . The modes corresponding to $n = 1249-1252$ are the corner states appearing at $E = 0$, denoted by red. The bulk and edge states are shown in blue and green, respectively. (c) Spatial profile of the pumped corner state corresponding to $n = 1251$. (d) Schematic diagram of the optical parametric scattering processes in the system. First polaritons from the pumped corner state scatter to edge states (black arrows) and then the polaritons from the edge states scatter back to the adjacent corner state (red arrows). Parameters: $J' = 5, \Delta = 0$.

exchange of information among themselves. To do this we consider all terms as described in Eq. (2) and take F_i as proportional to the amplitudes in each micropillar corresponding to one of the corner states, i.e., $F_i = f_s \psi_i^{(c)}$, where $\psi^{(c)}$ is the corner state eigenfunction. We choose the pump profile with the same spatial profile as the eigenstate corresponding to $n = 1251$, shown in Fig. 1(c), and also for simplicity we fix $\Gamma/2 = P$. With the proper choice of parameters, we consider parametric instability in the system where pairs of polaritons from this corner state can scatter to the edge modes while conserving energy. This regime of optical parametric oscillation (OPO) was previously deeply studied in planar microcavities [65–69]. Due to secondary parametric scattering processes [70,71], we expect that the edge states will couple to another corner. In this way with the help of the edge states we can nonlinearly couple the two corners, as described by the schematic Fig. 1(d).

Parametric instability.—To investigate parametric instability we first drive the system to a steady state, which is obtained by solving Eq. (2), and then study the behaviour of linear (Bogoliubov) fluctuations

$$\psi_i = \psi_{(0,i)} + u_i e^{-i\omega t} + v_i^* e^{i\omega^* t}, \quad (3)$$

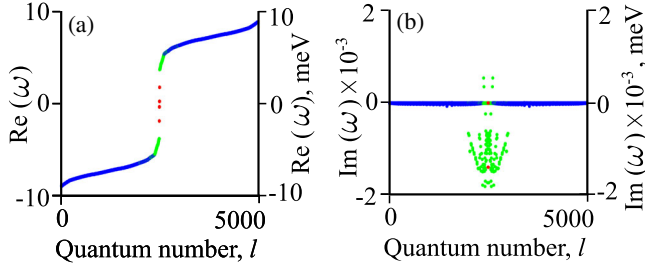


FIG. 2. Real and imaginary parts of the eigenvalues of the fluctuations as a function of quantum number l in (a) and (b) respectively. The states located at the corners are shown in red. The bulk and the edge states are represented by blue and green dots, respectively. Note that the total eight states corresponding to the four corners are in the band gap in (a). The positive imaginary part implies instability in the system and in the real space those four states having $\text{Im}(\omega) > 0$ correspond to different edge states. This also indicates that the pumped corner state couples to more than one edge state. Parameters: $J' = 5$, $\Delta = -0.3$, $\alpha_{\text{NL}} = 0.2$, $f_s = \sqrt{1.4}$.

ψ_0 is the stationary solution of Eq. (2), which essentially takes the form of the driven corner state; u and v are spatial functions of the fluctuations. $\psi_{(0,i)}$ is value of the ψ_0 at the lattice site i . Similarly u_i and v_i are the amplitudes of fluctuations at lattice site i . Here ω is the frequency of the fluctuations, which is in general complex to encapsulate the instabilities of the system. Substituting Eq. (3) into Eq. (2), we obtain the following eigenvalue equations

$$\begin{aligned} \omega u_i &= (iP' + \Delta')u_i + \sum_{(j)} J_{ij}u_j + (1 - i\alpha_{\text{NL}})\psi_{(0,i)}^2 v_i, \\ \omega v_i &= (iP' - \Delta')v_i - \sum_{(j)} J_{ij}v_j - (1 + i\alpha_{\text{NL}})(\psi_{(0,i)}^*)^2 u_i, \end{aligned} \quad (4)$$

where $\Delta' = \Delta + 2|\psi_{(0,i)}|^2$ and $P' = P - (\Gamma/2) - 2\alpha_{\text{NL}}|\psi_{(0,i)}|^2$. The eigenvalues of Eq. (4) are plotted as a function of the quantum number l of the fluctuation in Fig. 2. The modes corresponding to $\text{Im}(\omega) > 0$ indicate instability in the system and these modes correspond to edge states when plotted in real space [61]. Thus, polariton-polariton scattering induces coupling between the corner mode and edge modes.

Corner-corner coupling mediated via parametric interaction.—Now instead of depending on the linear Bogoliubov theory we directly simulate the dynamics of the system described by Eq. (2) starting from an initial vacuum state corresponding to a zero mean field. At each time step, the solution can be expanded as a linear superposition of the eigenstates of the linear system as

$$\psi_i(t) = \sum_n C_n(t)\psi_{(n,i)}, \quad (5)$$

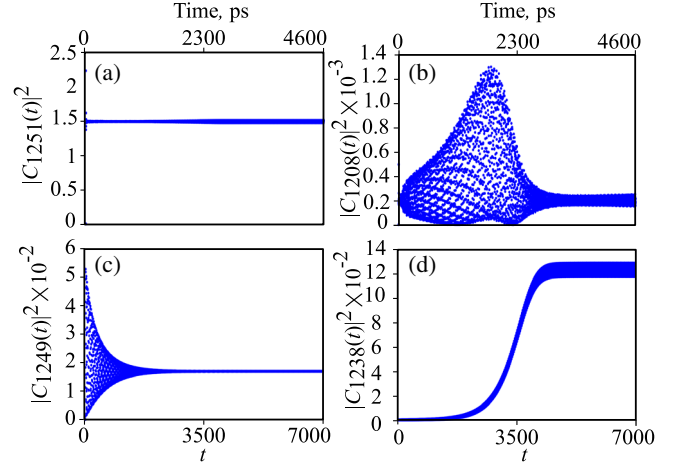


FIG. 3. The overlap $|C_n(t)|^2$ as a function of time for (a) the excited corner, $n = 1251$, (b) the edge state corresponding to $n = 1208$, and (c) the adjacent corner, $n = 1249$. (d) In later time, due to higher order terms, another edge state corresponding to $n = 1238$ appears in the system. The nonzero value of intensity of the adjacent corner indicates that both the corners are coupled.

where $C_n(t) = \sum_i \psi_i(t)\psi_{(n,i)}^*$. Physically $|C_n(t)|^2$ represents the intensity (or overlap) of each eigenstate. A plot of $|C_n(t)|^2$ as a function of time is shown in Fig. 3 for n corresponding to the excited corner, edge states, and another adjacent corner state. Figure 3(a) shows that in a very short time (much faster than the chosen range in the time plotted), the excited corner reaches its steady state and starts to couple to the edge states as shown in Fig. 3(b). Note that the excited corner state couples with more than one edge state and they have different intensity profiles with time (here as an example we have plotted only one). In Fig. 3(c) the intensity profile of the adjacent corner is plotted with time and the nonzero value indicates that there is coupling between the two corners. Without the nonlinear terms, the coupling of the excited corner state to the edge states or its adjacent corner state vanishes [61]. In a later time we observe significant intensity corresponding to another edge state as shown in Fig. 3(d), which eventually has no effect on the steady adjacent corner state.

The possibility that the nonlinear terms directly couple the corner states can not be discarded from the obtained results so far. However the analysis of the linear fluctuations can be repeated in the eigenbasis. Doing this in the Supplemental Material [61], we find that there is no parametric instability of a corner state into another corner state but only into the edge states. Thus, we ascertain that polaritons from the pumped corner mode couple first to an adjacent edge mode and it is via this edge mode that coupling to the adjacent corner mode is achieved.

The most important parameters in our scheme to realize the coupling are the nonlinear interaction and loss terms. Here the nonlinear self-energy in the system becomes about 1.36 meV, which is within experimental limits [72]. We have

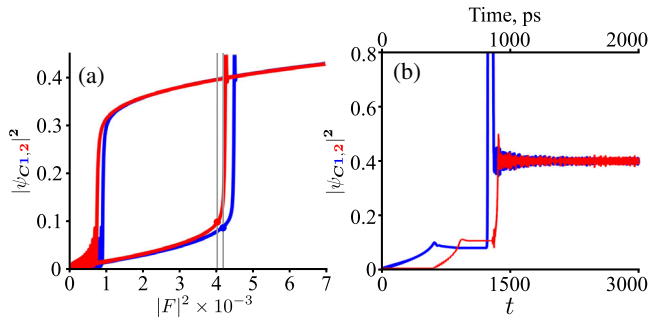


FIG. 4. (a) Hysteresis curve of polariton density vs pump power for the two corner sites (C1 and C2). For the following plots we fix the value of the pump at each site to the intensity indicated by the vertical gray lines. (b) Time dynamics of the corner sites, C1 and C2 in the presence of a continuous pump at both corners and pulse at C1 (which is gradually turned on to avoid unwanted jumps in the initial stages). A pulse switches C1 from the lower to upper intensity state and then due to the parametric scattering, C2 is also switched. We consider that the frequencies of both pumps and the central pulse frequency are the same. All the blue curves correspond to C1 and red curves correspond to C2. Parameters: $\Delta = -0.3$, $F_0 = 33$, $x_0 = 1$, $y_0 = 1$, $L = 1$, $t_0 = 1283$, $\tau = 15$.

taken the nonlinear loss coefficient as $\alpha_{\text{NL}} = 0.2$, where a similar value was used in Ref. [73].

Demonstration of transfer of binary information.—Here we demonstrate that the coupling between corners mediated by parametric instability is sufficient to transfer binary information. Such demonstration is based on using near-resonant coherent laser fields at each corner to place them in a bistable regime, which forces each corner state to either be in a low or high intensity state. Switching the state of one corner results in a later switch of the adjacent corner state, corresponding to a transfer of information. Remarkably, this can occur even in the presence of a realistic level of disorder.

To show bistability we consider Eq. (2) with the pump profile of the eigenstate $n = 1251$ and $n = 1249$, respectively, and slowly vary the intensity of the pump in time (over 9000 units ~ 6000 ps). The intensity corresponding to the corner sites (C1 and C2) as a function of pump intensity is plotted in Fig. 4(a), where the characteristic hysteresis loops show that bistability is present (different corners are nonidentical due to the lack of symmetry of the underlying lattice, which is why the hysteresis curves are slightly different). Gradually increasing the pump intensity to the level marked by the vertical grey lines in Fig. 4(a), allows each corner state to be initialized in its lower intensity state. Next, we apply a coherent Gaussian shaped pulse at corner C1 of the form $F = F_0 \exp\{-(x - x_0)^2 + (y - y_0)^2\}/L^2 - (t - t_0)^2/\tau^2 - i\omega_p t\}$, where F_0 is the amplitude of the pulse which is launched at (x_0, y_0) , the coordinates of C1; L and τ are the widths of the pulse in space and time. The time dynamics of both the corner sites in presence of the pumps and pulse is plotted in Fig. 4(b), which shows that the pulse switches C1 from its lower state to the upper

state and then due to the parametric scattering, C2 also switches to the upper intensity state. The same switching does not occur in the absence of the pump at C1, that is, it is only when the first corner supports bistability that a binary signal can be transported and not just a direct effect of the applied pulse [61].

All the calculations in this section were performed considering also an on site disorder with uniform distribution and peak to peak magnitude of 0.03. This, physically corresponds to a disorder strength of $30 \mu\text{eV}$ (for $J = 1 \text{ meV}$), which has been recorded experimentally [63].

Advantage of topological corner states over regular square lattice.—One could imagine that a similar scheme of coupling could occur in nontopological systems. However we have found that for similar parameters, a regular square lattice operates much slower, not reaching a steady state even after 5000 ps in the Supplemental Material [61]. This is understandable from the fact that, in the considered scheme, the linear decay is compensated by a nonresonant pump and the only dissipation present is the nonlinear decay ($\alpha_{\text{NL}}|\psi|^2\psi$). Since the regular square lattice does not show any localized mode (all the modes are distributed over many sites), for a particular site the decay $\alpha_{\text{NL}}|\psi|^2\psi$ becomes very weak and consequently the corner site reaches a steady state very slowly. On the other hand, since the topological corner modes are perfectly localized at the corners, this problem does not arise. To solve this, we added some linear decay in the system, which indeed made the system attain a steady state faster, but we did not observe bistability in the case of a regular square lattice within the same window of pump intensity (or in fact a larger intensity window either). Bistability did occur in the lattice with corner modes in presence of linear loss. In this case polaritons are localized and experience a stronger nonlinear interaction than the case of delocalized polaritons in a regular square lattice that automatically spread out over a wider area. In other words, the advantage of the scheme with topological corner states over a regular lattice is faster operation with lower power.

Conclusions.—We considered the appearance of topologically protected corner states in a square array of coupled exciton-polariton micropillars. These systems can be distinguished from other topological photonic systems by the presence of significant nonlinearity arising from polariton-polariton scattering. Here we found that such processes allow corner states to be nonlinearly coupled to edge states, which can be further coupled to adjacent corner states. That is, in the nonlinear regime, edge states act as intermediaries between corners. It is generally speculated that topological modes can be relevant in information processing and we anticipate that the ability to couple multiple topological modes in a single system will be essential to such directions [74,75].

We thank Sanjib Ghosh and Kevin Dini for helpful discussions and comments. The work was supported by the Ministry of Education, Singapore (Grant No. M0E2017-T2-1-001).

*Corresponding author.

rimi001@e.ntu.edu.sg

†Corresponding author.

tchliew@gmail.com

- [1] M. Z. Hasan and C. L. Kane, *Rev. Mod. Phys.* **82**, 3045 (2010).
- [2] X.-L. Qi and S.-C. Zhang, *Rev. Mod. Phys.* **83**, 1057 (2011).
- [3] F. D. M. Haldane and S. Raghu, *Phys. Rev. Lett.* **100**, 013904 (2008).
- [4] Z. Wang, Y. D. Chong, J. D. Joannopoulos, and M. Soljacic, *Phys. Rev. Lett.* **100**, 013905 (2008).
- [5] M. Hafezi, E. A. Demler, M. D. Lukin, and J. M. Taylor, *Nat. Phys.* **7**, 907 (2011).
- [6] Z. Wang, Y. D. Chong, J. D. Joannopoulos, and M. Soljacic, *Nature (London)* **461**, 772 (2009).
- [7] M. Hafezi, S. Mittal, J. Fan, A. Migdall, and J. M. Taylor, *Nat. Photonics* **7**, 1001 (2013).
- [8] Y. Poo, R. X. Wu, Z. Lin, Y. Yang, and C. T. Chan, *Phys. Rev. Lett.* **106**, 093903 (2011).
- [9] M. C. Rechtsman, J. M. Zeuner, Y. Plotnik, Y. Lumer, D. Podolsky, F. Dreisow, S. Nolte, M. Segev, and A. Szameit, *Nature (London)* **496**, 196 (2013).
- [10] W. J. Chen, S. J. Jiang, X. D. Chen, B. Zhu, L. Zhou, J. W. Dong, and C. T. Chan, *Nat. Commun.* **5**, 5782 (2014).
- [11] G. Jotzu, M. Messer, R. Desbuquois, M. Lebrat, T. Uehlinger, D. Greif, and T. Esslinger, *Nature (London)* **515**, 237 (2014).
- [12] M. Aidelsburger, M. Lohse, C. Schweizer, M. Atala, J. T. Barreiro, S. Nascimbene, N. R. Cooper, I. Bloch, and N. Goldman, *Nat. Phys.* **11**, 162 (2015).
- [13] C.-E. Bardyn, T. Karzig, G. Refael, and T. C. H. Liew, *Phys. Rev. B* **91**, 161413(R) (2015).
- [14] A. V. Nalitov, D. D. Solnyshkov, and G. Malpuech, *Phys. Rev. Lett.* **114**, 116401 (2015).
- [15] T. Karzig, C.-E. Bardyn, N. H. Lindner, and G. Refael, *Phys. Rev. X* **5**, 031001 (2015).
- [16] S. Klembt, T. H. Harder, O. A. Egorov, K. Winkler, R. Ge, M. A. Bandres, M. Emmerling, L. Worschech, T. C. H. Liew, M. Segev, C. Schneider, and S. Hofling, *Nature (London)* **562**, 552 (2018).
- [17] Y. V. Kartashov and D. V. Skryabin, *Phys. Rev. Lett.* **119**, 253904 (2017).
- [18] R. Banerjee, T. C. H. Liew, and O. Kyriienko, *Phys. Rev. B* **98**, 075412 (2018).
- [19] Z. Yang, F. Gao, X. Shi, X. Lin, Z. Gao, Y. Chong, and B. Zhang, *Phys. Rev. Lett.* **114**, 114301 (2015).
- [20] R. Fleury, A. B. Khanikaev, and A. Alu, *Nat. Commun.* **7**, 11744 (2016).
- [21] W. A. Benalcazar, B. A. Bernevig, and T. L. Hughes, *Science* **357**, 61 (2017).
- [22] W. A. Benalcazar, B. Andrei Bernevig, and T. L. Hughes, *Phys. Rev. B* **96**, 245115 (2017).
- [23] Z. Song, Z. Fang, and C. Fang, *Phys. Rev. Lett.* **119**, 246402 (2017).
- [24] J. Langbehn, Y. Peng, L. Trifunovic, F. von Oppen, and P. W. Brouwer, *Phys. Rev. Lett.* **119**, 246401 (2017).
- [25] F. Schindler, A. M. Cook, M. G. Vergniory, Z. Wang, S. S. P. Parkin, B. Andrei Bernevig, and T. Neupert, *Sci. Adv.* **4**, eaat0346 (2018).
- [26] M. S.-Garcia, V. Peri, R. Susstrunk, O. R. Bilal, T. Larsen, L. G. Villanueva, and S. D. Huber, *Nature (London)* **555**, 342 (2018).
- [27] S. Imhof, C. Berger, F. Bayer, J. Brehm, L. W. Molenkamp, T. Kiessling, F. Schindler, C. H. Lee, M. Greiter, T. Neupert, and R. Thomale, *Nat. Phys.* **14**, 925 (2018).
- [28] C. W. Peterson, W. A. Benalcazar, T. L. Hughes, and G. A. Bahl, *Nature (London)* **555**, 346 (2018).
- [29] M. Ezawa, *Phys. Rev. Lett.* **120**, 026801 (2018).
- [30] B. Y. Xie, H. F. Wang, H.-X. Wang, X. Y. Zhu, J.-H. Jiang, M. H. Lu, and Y. F. Chen, *Phys. Rev. B* **98**, 205147 (2018).
- [31] J. Noh, W. A. Benalcazar, S. Huang, M. J. Collins, K. Chen, T. L. Hughes, and M. C. Recheckman, *Nat. Photonics* **12**, 408 (2018).
- [32] H. Xue, Y. Yang, F. Gao, Y. Chong, and B. Zhang, *Nat. Mater.* **18**, 108 (2019).
- [33] M. Geier, L. Trifunovic, M. Hoskam, and P. W. Brouwer, *Phys. Rev. B* **97**, 205135 (2018).
- [34] M. Ezawa, *Phys. Rev. B* **98**, 201402(R) (2018).
- [35] F. K. Kunst, G. van Miert, and E. J. Bergholtz, *Phys. Rev. B* **97**, 241405(R) (2018).
- [36] H. Araki, T. Mizoguchi, and Y. Hatsugai, *Phys. Rev. B* **99**, 085406 (2019).
- [37] X. Ni, M. Weiner, Andrea Alu, and A. B. Khanikaev, *Nat. Mater.* **18**, 113 (2019).
- [38] F. F. Li, H. X. Wang, Z. Xiong, Q. Lou, P. Chen, R. X. Wu, Y. Poo, J. H. Jiang, and S. John, *Nat. Commun.* **9**, 2462 (2018).
- [39] R. Susstrunk and S. D. Huber, *Science* **349**, 47 (2015).
- [40] L. M. Nash, D. Kleckner, Al. Read, V. Vitelli, A. M. Turner, and W. T. M. Irvine, *Proc. Natl. Acad. Sci. U.S.A.* **112**, 14495 (2015).
- [41] X.-D. Chen, W.-M. Deng, F.-L. Shi, F.-L. Zhao, M. Chen, and J.-W. Dong, *Phys. Rev. Lett.* **122**, 233902 (2019).
- [42] A. E. Hassan, F. K. Kunst, A. Moritz, G. Andler, E. J. Bergholtz, and M. Bourennane, *Nat. Photonics* **13**, 697 (2019).
- [43] A. B.-Redondo, B. Bell, D. Oren, B. J. Eggleton, and M. Segev, *Science* **362**, 568 (2018).
- [44] J. L. Tambasco, G. Corrielli, R. J. Chapman, A. Crespi, O. Zilberberg, R. Osellame, and A. Peruzzo, *Sci. Adv.* **4**, eaat3187 (2018).
- [45] Y. Wang, X.-Ling Pang, Y.-Heng Lu, J. Gao, Z.-Qiang Jiao, H. Tang, and X.-Min Jin, *arXiv:1810.01435*.
- [46] Y. Yang, Z. Jia, Y. Wu, Z. H. Hang, H. Jiang, and X. C. Xie, *arXiv:1903.01816*.
- [47] H. Deng, H. Haug, and Y. Yamamoto, *Rev. Mod. Phys.* **82**, 1489 (2010).
- [48] I. Carusotto and C. Ciuti, *Rev. Mod. Phys.* **85**, 299 (2013).
- [49] S. R. K. Rodriguez, A. Amo, I. Sagnes, L. Le. Gratiet, E. Galopin, A. Lemaitre, and J. Bloch, *Nat. Commun.* **7**, 11887 (2016).
- [50] M. Milicevic, T. Ozawa, P. Andreakou, I. Carusotto, T. Jacqmin, E. Galopin, A. Lemaitre, L. Le. Gratiet, I. Sagnes, J. Bloch, and A. Amo, *2D Mater.* **2**, 034012 (2015).
- [51] V. G. Sala, D. D. Solnyshkov, I. Carusotto, T. Jacqmin, A. Lemaitre, H. Tercas, A. Nalitov, M. Abbarchi, E. Galopin, I. Sagnes, J. Bloch, G. Malpuech, and A. Amo, *Phys. Rev. X* **5**, 011034 (2015).
- [52] K. Winkler, O. A. Egorov, I. G. Savenko, X. Ma, E. Estrecho, T. Gao, S. Muller, M. Kamp, T. C. H. Liew, E. A. Ostrovskaya, S. Hofling, and C. Schneider, *Phys. Rev. B* **93**, 121303(R) (2016).

- [53] S. Klembt, T. H. Harder, O. A. Egorov, K. Winkler, H. Suchomel, J. Beierlein, M. Emmerling, C. Schneider, and S. Hofling, *Appl. Phys. Lett.* **111**, 231102 (2017).
- [54] B. Zhang, S. Brodbeck, Z. Wang, M. Kamp, C. Schneider, S. Hofling, and H. Deng, *Appl. Phys. Lett.* **106**, 051104 (2015).
- [55] O. Bleu, D. D. Solnyshkov, and G. Malpuech, *Phys. Rev. B* **93**, 085438 (2016).
- [56] Y. V. Kartashov and D. V. Skryabin, *Optica* **3**, 1228 (2016).
- [57] D. R. Gulevich, D. Yudin, D. V. Skryabin, I. V. Iorsh, and I. A. Shelykh, *Sci. Rep.* **7**, 1780 (2017).
- [58] C. Li, F. Ye, X. Chen, Y. V. Kartashov, A. Ferrando, L. Torner, and Dmitry V. Skryabin, *Phys. Rev. B* **97**, 081103(R) (2018).
- [59] S. Mandal, R. Ge, and T. C. H. Liew, *Phys. Rev. B* **99**, 115423 (2019).
- [60] R. Keil, C. Poli, M. Heinrich, J. Arkininstall, G. Weihs, H. Schomerus, and A. Szameit, *Phys. Rev. Lett.* **116**, 213901 (2016).
- [61] See Supplemental Material at <http://link.aps.org/supplemental/10.1103/PhysRevLett.124.063901> for the energy eigenvalues and eigenstates as a function of quantum number n in the continuous model using exciton polariton micropillars, for the spatial profile of the instable modes of Fig. 2(b), for the clarification that this coupling is an effect of nonlinearity, for the proof that there is no direct coupling between corner modes, for the proof that the applied pulse alone cannot switch the another corner C_2 , and for the comparison of bistability of the topological corner mode over the regular square lattice, which includes Refs. [60,62,63].
- [62] M. Galbiati, L. Ferrier, D. D. Solnyshkov, D. Tanese, E. Wertz, A. Amo, M. Abbarchi, P. Senellart, I. Sagnes, A. Lemaître, E. Galopin, G. Malpuech, and J. Bloch, *Phys. Rev. Lett.* **108**, 126403 (2012).
- [63] F. Baboux, L. Ge, T. Jacqmin, M. Biondi, E. Galopin, A. Lemaître, L. Le Gratiet, I. Sagnes, S. Schmidt, H. E. Tureci, A. Amo, and J. Bloch, *Phys. Rev. Lett.* **116**, 066402 (2016).
- [64] S. Michaelis de Vasconcellos, A. Calvar, A. Dousse, J. Suffczynski, N. Dupuis, A. Lemaître, I. Sagnes, J. Bloch, P. Voisin, and P. Senellart, *Appl. Phys. Lett.* **99**, 101103 (2011).
- [65] C. Ciuti, P. Schwendimann, and A. Quattropani, *Semicond. Sci. Technol.* **18**, S279 (2003).
- [66] C. Ciuti, P. Schwendimann, and A. Quattropani, *Phys. Rev. B* **63**, 041303(R) (2001).
- [67] D. M. Whittaker, *Phys. Rev. B* **63**, 193305 (2001).
- [68] R. M. Stevenson, V. N. Astratov, M. S. Skolnick, D. M. Whittaker, M. Emam-Ismaïl, A. I. Tartakovskii, P. G. Savvidis, J. J. Baumberg, and J. S. Roberts, *Phys. Rev. Lett.* **85**, 3680 (2000).
- [69] C. Ciuti and I. Carusotto, *Phys. Status Solidi B* **242**, 2224 (2005).
- [70] P. G. Savvidis, C. Ciuti, J. J. Baumberg, D. M. Whittaker, M. S. Skolnick, and J. S. Roberts, *Phys. Rev. B* **64**, 075311 (2001).
- [71] A. I. Tartakovskii, D. N. Krizhanovskii, D. A. Kurysh, V. D. Kulakovskii, M. S. Skolnick, and J. S. Roberts, *Phys. Rev. B* **65**, 081308(R) (2002).
- [72] Y. Sun, Y. Yoon, M. Steger, G. Liu, L. N. Pfeiffer, K. West, D. W. Snoke, and K. A. Nelson, *Nat. Phys.* **13**, 870 (2017).
- [73] J. Keeling and N. G. Berloff, *Phys. Rev. Lett.* **100**, 250401 (2008).
- [74] H. Flayac and I. G. Savenko, *Appl. Phys. Lett.* **103**, 201105 (2013).
- [75] D. Ballarini, M. De Giorgi, E. Cancellieri, R. Houdre, E. Giacobino, R. Cingolani, A. Bramati, G. Gigli, and D. Sanvitto, *Nat. Commun.* **4**, 1778 (2013).